Syntheses, Structures and Electrochemical Properties of Two New Copper(II) Complexes Based on Isomeric Bis(pyridylformyl)piperazine Ligands and Rigid/Flexible Organic Dicarboxylates

Hong-Yan Lin, Peng Liu, Xiu-Li Wang, Chuang Xu, and Guo-Cheng Liu

Department of Chemistry, Bohai University, Jinzhou, 121000, P. R. China

Reprint requests to Prof. Xiu-Li Wang. E-mail: wangxiuli@bhu.edu.cn

Z. Naturforsch. **2013**, *68b*, 138 – 146 / DOI: 10.5560/ZNB.2013-2291
Received November 1, 2012

Two new copper(II) complexes, $[Cu_2(3\text{-bpfp})(2,6\text{-PDA})_2(H_2O)_2]$ (**1**) and $[Cu(4\text{-bpfp})_{0.5}(glu)]\cdot H_2O$ (**2**), have been hydrothermally synthesized by self-assembly of isomeric bis(pyridylformyl)piperazine ligands [3-bpfp = bis(3-pyridylformyl)piperazine, 4-bpfp = bis(4-pyridylformyl)piperazine], rigid pyridine-2,6-dicarboxylic acid (2,6-H_2PDA) or flexible glutaric acid (H_2glu), and copper(II) chloride. Single-crystal X-ray diffraction analysis reveals that two adjacent Cu^{II} ions are connected by the 3-bpfp ligand to build a dinuclear unit in complex **1**, in which 2,6-PDA serves as a terminal chelating ligand. Adjacent dinuclear units are further linked by hydrogen bonding and π-π stacking interactions to form a three-dimensional (3D) supramolecular network. Complex **2** is a 3D coordination polymeric framework based on a layer polymer $[Cu(glu)]_n$ and bridging 4-bpfp ligands with 6-connected ($4^4.6^{10}.8$) topology. In **1** and **2**, the ligands 3-bpfp and 4-bpfp adopt a μ_2-bridging coordination mode (*via* ligation of pyridyl nitrogen atoms). The thermal stability and the electrochemical properties of the title complexes have been studied.

Key words: Bis(pyridylformyl)piperazine Ligand, Organic Dicarboxylate, Copper(II) Complex, Crystal Structure, Electrochemical Properties

Introduction

The rational assembly of high-dimensional coordination complexes or supramolecular architectures based on metal ions (or metal clusters) and organic ligands has attracted much attention in crystal engineering in recent years [1 – 4]. Generally, high-dimensional supramolecular networks can be obtained by connecting polynuclear discrete subunits or low-dimensional entities *via* non-covalent interactions such as hydrogen bonding and π-π stacking [5 – 7]. In this case, the proper selection of organic ligands might be the key step to obtain the expected complexes. Rigid aromatic dicarboxylates as *O*-donor ligands [such as 1,2-benzenedicarboxylic, 1,3-benzenedicarboxylic and pyridine-2,6-dicarboxylic acid (2,6-H_2PDA)], have been extensively employed to construct coordination frameworks that exhibit diverse structures with potential applications as functional materials [8 – 11]. Compared with aromatic dicarboxylic acids, flexible aliphatic dicarboxylic acids (such as succinic acid, glutaric acid(H_2glu), hexane dicarboxylic acid) have received less attention. These ligands may lead to intriguing structural motifs due to their ability to adopt numerous energetically similar conformations [12 – 15].

The structural complexity in metal-dicarboxylate frameworks can been enhanced through the introduction of neutral *N*-donor ligands such as bispyridyls, which can connect metal ions through their nitrogen atoms into novel structures with interesting physicochemical properties [16 – 19]. Recently, our group has reported a series of metal-organic coordination polymers constructed from aromatic polycarboxylic acids and various bispyridyl-type ligands [20 – 24]. Using two isomeric bis(pyridylformyl)piperazine ligands [3-bpfp = bis(3-pyridylformyl)piperazine), 4-bpfp = bis(4-pyridylformyl)piperazine)] and aromatic polycarboxylate ligands, a novel 3,5-connected binodal three-dimensional framework $[Cu(3\text{-bpfp})(HBTC)]\cdot H_2O$($H_3$BTC = 1,3,5-benzenetricarboxylate) with $(4.5^3.8^2.9^4)_3(4.5^2)_2$ topology, and the layer structures

$[Cu_2(3\text{-bpfp})(BDC)_2(H_2O)_2]\cdot 4H_2O$ and $[Cu(4\text{-bpfp})_{0.5}(HBTC)(H_2O)]$ have been obtained [25].

We have tried to extend our previous work by employing bis(3-pyridylformyl)piperazine (3-bpfp) and bis(4-pyridylformyl)piperazine (4-bpfp) as neutral *N*-donor ligands, following the limited studies of coordination polymers based on these two ligands [26–31]. Two new copper complexes, $[Cu_2(3\text{-bpfp})(2,6\text{-PDA})_2(H_2O)_2]$ (**1**) and $[Cu(4\text{-bpfp})_{0.5}(glu)]\cdot H_2O$ (**2**), have been prepared from the isomeric ligands 3-bpfp/4-bpfp and the bicarboxylate ligands derived from the rigid 2,6-H_2PDA or flexible H_2glu under hydrothermal conditions. The thermal stability and the electrochemical properties of the title complexes have been investigated.

Results and Discussion

*Crystal and molecular structure of $[Cu_2(3\text{-bpfp})(2,6\text{-PDA})_2(H_2O)_2]$ (**1**)*

The single-crystal X-ray diffraction study has revealed that compound **1** is a 3D supramolecular network based on binuclear copper units composed of 3-bpfp and 2,6-PDA ligands. The coordination environment of the Cu atoms is shown in Fig. 1. The Cu atom is penta-coordinated by two oxygen atoms belonging to two carboxyl groups from one 2,6-PDA ligand (Cu1–O2 2.0324(18), Cu1–O5 2.0392(18) Å), one nitrogen atom from a bridging 3-bpfp ligand with a bond length of 1.9773(19) Å (Cu1–N1), one nitrogen atom from one 2,6-PDA ligand with a bond length of 1.9071(19) Å (Cu1–N2), and one oxygen atom O1W from a coordinated water molecule (Cu1–O1W = 2.224(2) Å), showing a distorted tetragonal pyramidal geometry.

2,6-PDA coordinates to one Cu atom with a nitrogen atom and two oxygen atoms from two carboxyl groups simultaneously, serving as a terminal ligand. Two adjacent Cu atoms are connected by the 3-bpfp ligand in the μ_2-bridging coordination mode to give a dinuclear structure, in which the two pyridyl rings of 3-bpfp are parallel and the non-bonding distance Cu···Cu is 13.21 Å.

Adjacent binuclear units are connected by O–H···O hydrogen bonding interactions to form a supramolecular layer, as shown in Fig. 2. The hydrogen bonds are formed between the carboxyl oxygen atoms (O1, O4) of 2,6-PDA and the oxygen atom (O1W) of the co-

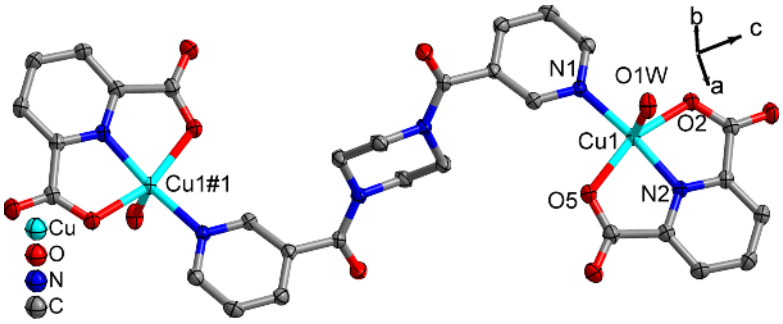

Fig. 1 (color online). The coordination environment of the Cu atoms in complex **1** (displacement ellipsoids at the 50% probability level). All H atoms and water molecules are omitted for clarity.

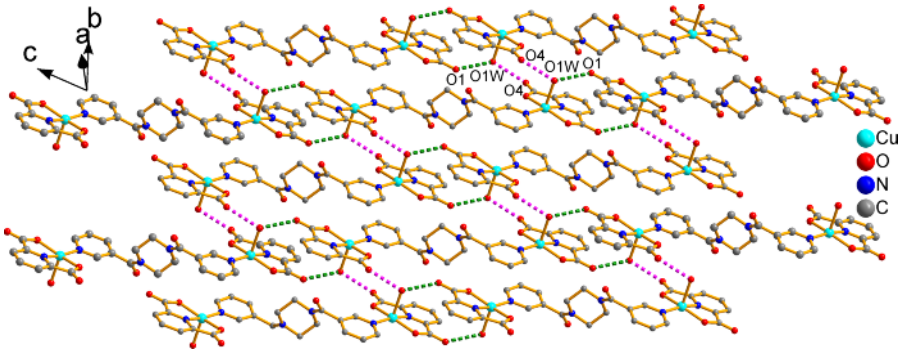

Fig. 2 (color online). The supramolecular layer of **1** formed by hydrogen bonding interactions (green and pink dotted lines: hydrogen bonds). All H atoms are omitted for clarity.

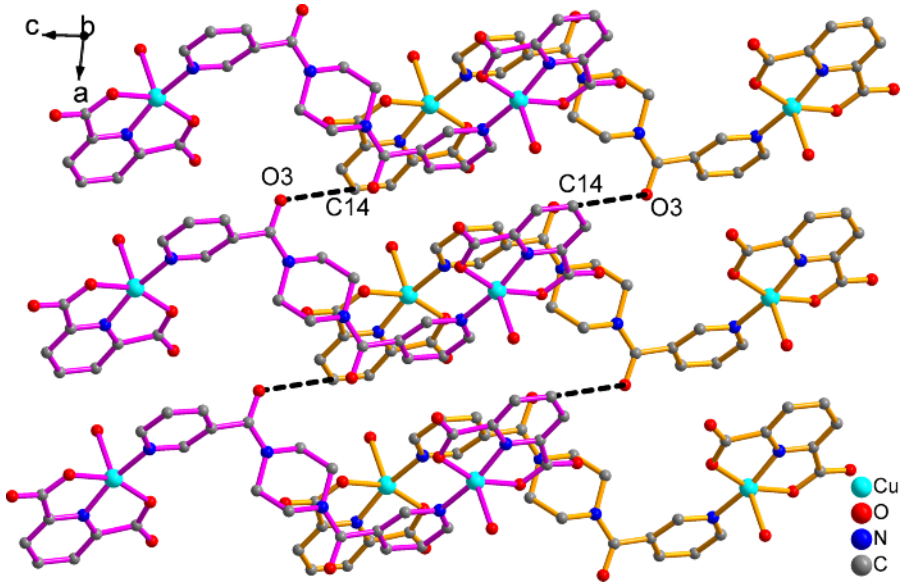

Fig. 3 (color online). 3D supramolecular network of complex **1** formed by hydrogen bonding and π-π stacking interactions (H atoms are omitted for clarity).

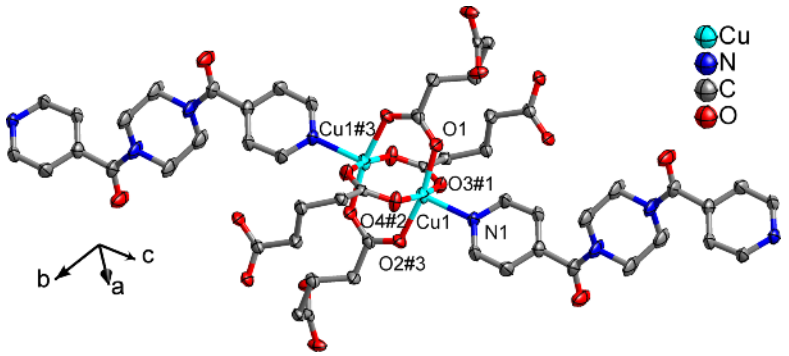

Fig. 4 (color online). The coordination environment of the Cu atoms in complex **2** (displacement ellipsoids 50 %). All H atoms and water molecules are omitted for clarity.

ordinated water molecule (O1···O1W = 2.808(3) Å). Adjacent layers are ultimately extended into a three-dimensional supramolecular network by weak C–H···O hydrogen bonds and π-π stacking interactions. The hydrogen bonds are formed between the carbon atom C14 of the pyridine ring of 3-bpfp and a carbonyl oxygen atom (O3) of 3-bpfp (C14···O3 = 2.716(3) Å). The π-π stacking interactions occur between pyridine rings of 3-bpfp ligands with face-to-face distances of *ca.* 3.61 Å (Fig. 3).

*Crystal and molecular structure of [Cu(4-bpfp)$_{0.5}$(glu)]·H$_2$O (**2**)*

The crystal and molecular structure of **2** has also been determined by single-crystal X-ray diffraction. Complex **2** is a 3D coordination polymer based on [Cu(glu)]$_n$ layers and bridging 4-bpfp ligands. The coordination environment of the Cu atom is shown in Fig. 4. Each Cu atom is five-coordinated by four carboxylic oxygen atoms from four glu ligands with Cu–O bond lengths ranging from 1.961(2) to 1.980(2) Å, and a pyridyl nitrogen atom of a 4-bpfp ligand with a Cu–N bond length of 2.163(3) Å. The two neighboring Cu atoms are connected by four carboxylic groups from four glu to form a dinuclear unit [Cu$_2$(-COO)$_4$]. Each glu adopts the bis(bidentate) coordination mode to link two dinuclear units, and each dinuclear unit is linked by four glu bridges to form a [Cu(glu)]$_n$ layer, as shown in Fig. 5a. In the layer, the non-bonding distances are 2.63 Å for Cu1#4···Cu1#5, 7.77 Å for Cu1#4···Cu1#6, 8.91 Å

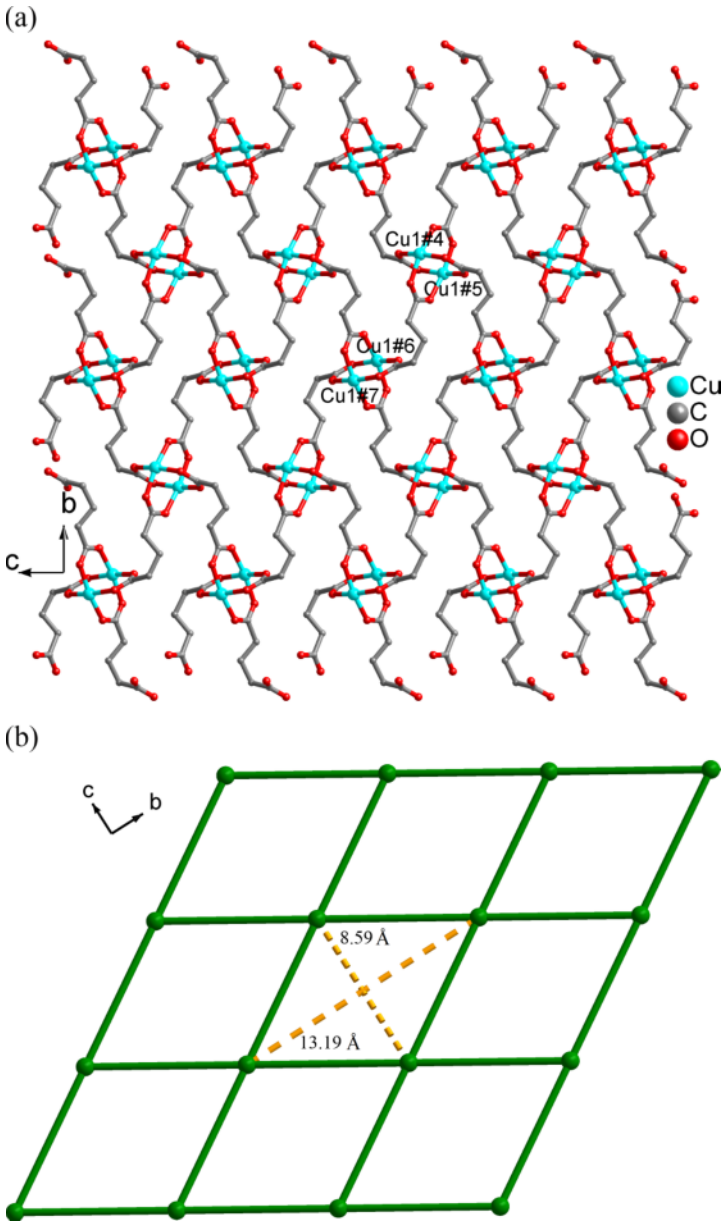

Fig. 5 (color online). (a) Layers in the cyrstal structure of complex **2** constructed by bridging ligands glu; (b) schematic representation of the layer of **2** in the *bc* plane (green balls, binuclear copper clusters; green lines, glu ligands).

for Cu1#4···Cu1#7, 6.88 Å for Cu1#5···Cu1#6, and 8.62 Å for Cu1#5···Cu1#7 (symmetry codes: #4 $-x$, $0.5+y$, $0.5-z$; #5 $-1+x$, $0.5-y$, $-1.5+z$; #6 $-1+x$, y, $-1+z$; #7 $-x$, $-y$, $1-z$). The average distance of the adjacent dinuclear units is 7.87 Å.

For a presentation of the connectivities in the solid-state structure of **2** the dinuclear units are taken as nodes and the glu ligands as linear linkers. The $[Cu(glu)]_n$ layer can thus be described as a 4-connected rhombic mesh (8.59 × 13.19 Å) network with $(4^4.6^2)$ topology (Fig. 5b). These layers are further connected by μ_2-bridging 4-bpfp ligands, resulting in the formation of a 3D coordination polymer network (Fig. 6a) with the non-bonding distance of dinuclear units of neighboring layers at 18.99 Å. Thus, each dinuclear

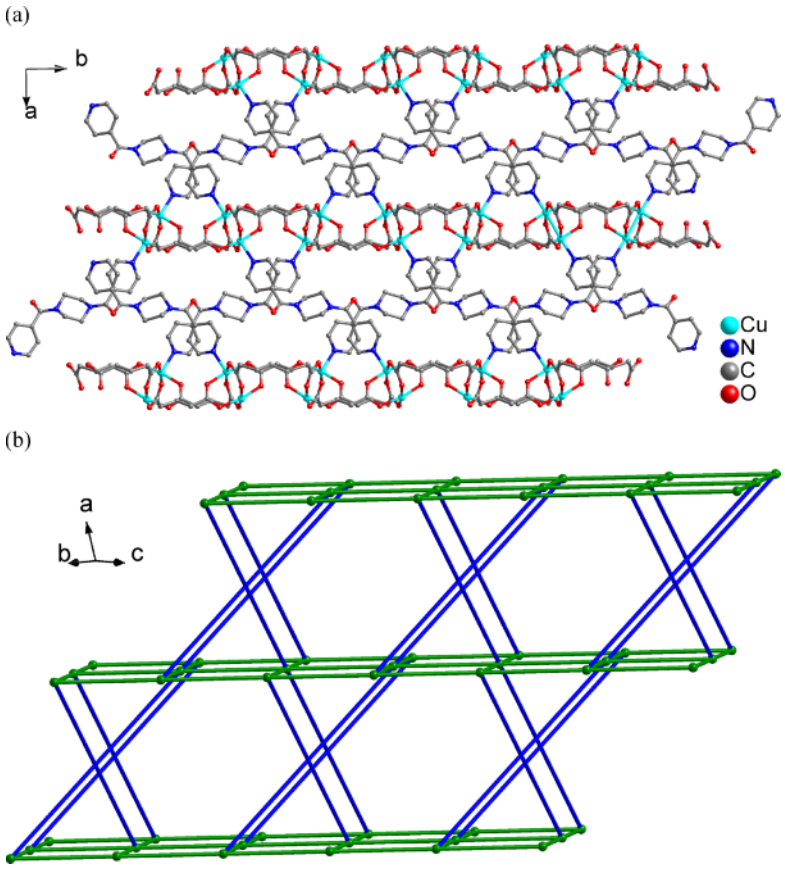

Fig. 6 (color online). (a) The 3D polymeric structure formed by ligands glu and 4-bpfp in the crystal structure of **2**; (b) schematic representation of the 3D network in **2** (green balls, binuclear copper clusters; green lines, glu ligands; blue lines, 4-bpfp ligands).

unit is surrounded by six organic ligands (four glu and two 4-bpfp ligands) and can simply be regarded as a 6-connected node. Both glu and 4-bpfp serve as linear linkers to connect two adjacent dinuclear units. Considering the dinuclear units as nodes and keeping the glu and 4-bpfp ligands as linkers, the overall 3D coordination polymer is best described as a unique 6-connected network with $(4^4.6^{10}.8)$ topology (Fig. 6b).

*Thermal properties of complexes **1** and **2***

The thermogravimetric (TG) analyses of the title complexes were conducted under N_2 atmosphere with a heating rate of 10 °C min^{-1} in the temperature range of 50 – 620 °C (Fig. 7). For complexes **1** and **2**, the TG curves exhibit two weight loss steps. The first one can be ascribed to the loss of water molecules: 5.3 % (calcd. 4.8 %) in **1** and 4.5 % (calcd. 5.0 %) in **2**. The second one occurs around 275 °C for **1** and 320 °C for **2**, and is to be attributed to the decomposition of the organic ligands. The remaining weight of 19.8 % for **1** and 22.7 % for **2** corresponds to the values calculated for CuO (calcd.: 20.3 % for **1**, 22.2 % for **2**).

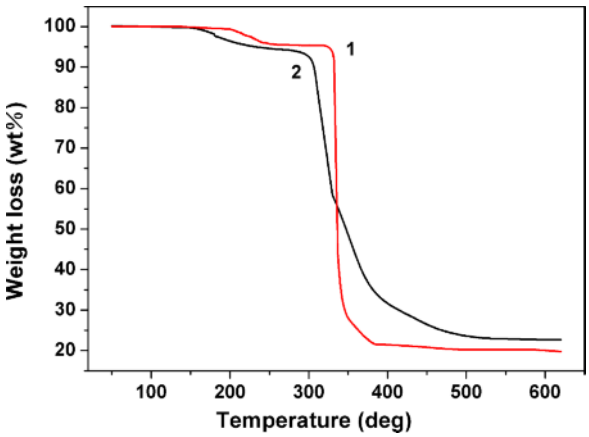

Fig. 7 (color online). Thermal gravimetric curves of **1** and **2**.

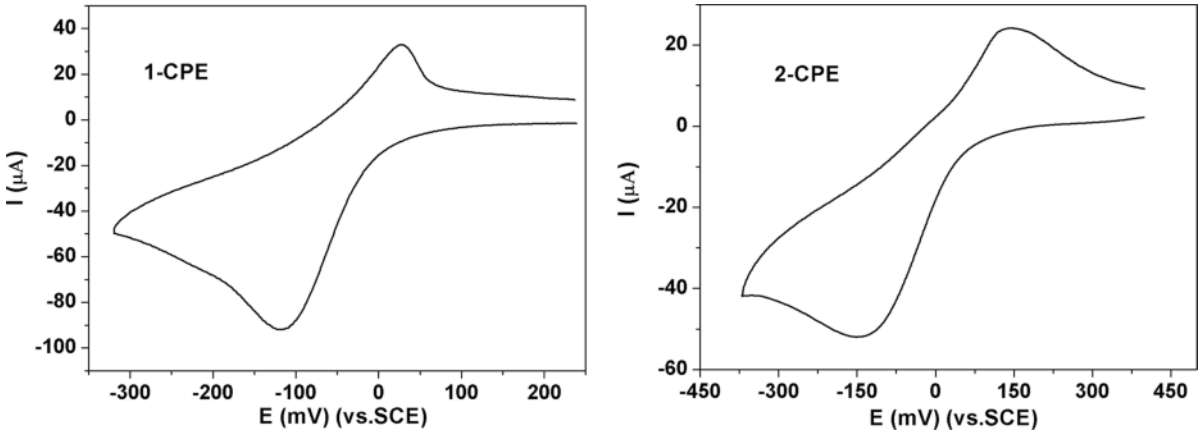

Fig. 8. Cyclic voltammograms of carbon paste electrodes bulk-modified by the title complexes (**1**-CPE and **2**-CPE) in 0.1 M H_2SO_4 aqueous solution. Scan rate: 60 mV s^{-1}.

*Electrochemical behavior of **1**-CPE and **2**-CPE*

As potential electrochemical and electrocatalytic materials, copper(II) complexes have the ability to undergo a reversible one-electron redox process [32, 33]. To study the redox properties of the title copper(II) complexes, carbon paste electrode bulk-modified with complexes **1** and **2** (**1**-CPE and **2**-CPE) were fabricated as working electrodes. The electrochemical behavior of **1**-CPE and **2**-CPE was studied in 0.1 M H_2SO_4 aqueous solution. As shown in Fig. 8, the cyclic voltammograms exhibit a quasi-reversible redox peak attributed to the redox couple of Cu^{II}/Cu^{I} in the potential range of 240 to −300 mV or 400 to −380 mV [32]. The mean peak potential $E_{1/2} = (E_{pa} + E_{pc})/2$ was −45 mV for **1**-CPE, and −5 mV for **2**-CPE. The difference of the peak potentials is caused by the different structures of the two copper(II) complexes.

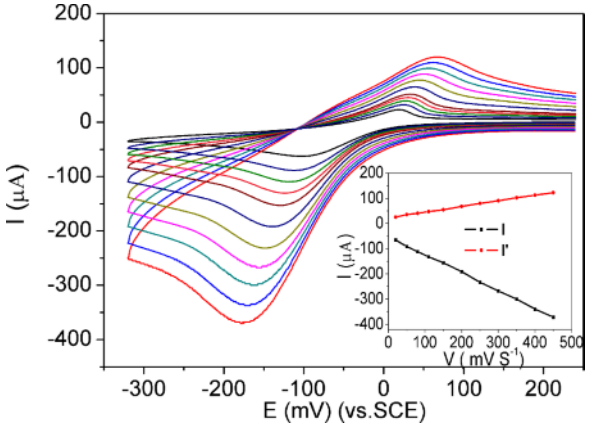

Fig. 9 (color online). Cyclic voltammograms of **1**-CPE in 0.1 M H_2SO_4 aqueous solution at different scan rates (from inner to outer) 20, 50, 80, 110, 150, 200, 250, 300, 350, 400, and 450 mV s^{-1}. The inset shows the plots of the anodic and cathodic peak currents *vs.* the scan rates.

1-CPE was used as an example, and the effect of scan rates on the electrochemical behavior in the potential range of +240 to −300 mV in 0.1 M H_2SO_4 aqueous solution was investigated (Fig. 9). With the scan rates increasing from 20 to 450 mV s^{-1}, the cathodic peak potentials shifted in the negative direction, while the corresponding anodic peak potentials shifted in the positive direction. The plots of peak currents *versus* scan rates are shown in the inset of Fig. 9. The anodic and the cathodic currents were proportional to the scan rates, which indicates that the redox process for **1**-CPE is surface-confined.

Conclusion

In summary, two new copper(II) complexes constructed with the bis-pyridyl-bis-amide ligands 3-bpfp and 4-bpfp and two different dicarboxylate ligands (rigid 2,6-H_2PDA or flexible H_2glu), $[Cu_2(3\text{-bpfp})(2,6\text{-PDA})_2(H_2O)_2]$ (**1**) and $[Cu(4\text{-bpfp})_{0.5}(glu)]\cdot H_2O$ (**2**), have been hydrothermally synthesized. In the two complexes, both 3-bpfp and 4-bpfp serve as bridging ligands and adopt the same μ_2-bridging coordination mode. The different coordination modes of the organic dicarboxylate ligands (2,6-H_2PDA and H_2glu) play an important role in governing the coordination motifs and the final

structures. The title complexes show well-defined redox properties. The preliminary results presented in this work suggest that the title complexes may be potential candidates for electrochemical materials.

Experimental Section

Materials and methods

Ligands 3-bpfp and 4-bpfp were synthesized by the literature method [34]. All other reagents employed were commercially available and used as received without further purification. Thermogravimetric analyses were performed with a Pyris Diamond TG-DTA instrument. FT-IR spectra (KBr pellets) were taken on a Magna FT-IR 560 spectrometer, and the elemental analyses (C, H, and N) were obtained from on a Perkin-Elmer 2400 CHN elemental analyzer. The electrochemical experiments were carried out with a CHI 440 electrochemical quartz crystal microbalance. A conventional three-electrode cell was used at room temperature. An SCE and a platinum wire were used as reference and auxiliary electrodes, respectively. The bulk modified CPEs (**1**-CPE and **2**-CPE) were fabricated following literature methods and taken as working electrodes [32].

*Synthesis of [Cu_2(3-bpfp)(2,6-PDA)$_2$(H_2O)$_2$] (**1**)*

A mixture of $CuCl_2{\cdot}2H_2O$ (0.034 g, 0.2 mmol), 2,6-H_2PDA (0.033 g, 0.2 mmol), 3-bpfp (0.032 g, 0.1 mmol), H_2O (12 mL), and NaOH (0.0144 g, 0.36 mmol) was stirred for 30 min in air, then transferred and sealed in a 25 mL Teflon reactor, which was heated at 120 °C for 4 d, leading to the formation of blue block-shaped crystals. These were washed with water and dried in air. Yield: ∼ 31 % (based on Cu). – Anal. for $C_{30}H_{26}Cu_2N_6O_{12}$: calcd. C 45.59, H 3.29, N 10.64; found C 45.45, H 3.35, N 10.78 %. – IR (KBr, cm^{-1}): ν = 3431 s, 2949 m, 2860 w, 2357 m, 2334 w, 1643 s, 1613 s, 1538 w, 1500 w, 1418 s, 1357 w, 1320 m, 1289 m, 1260 s, 1215 s, 1147 m, 1064 w, 1035 w, 1003 s, 906 w, 847 s, 757 s, 715 m, 667 m, 636 m, 607 w, 531 m.

*Synthesis of [Cu(4-bpfp)$_{0.5}$(glu)]·H_2O (**2**)*

A mixture of $CuCl_2{\cdot}2H_2O$ (0.034 g, 0.2 mmol), H_2glu (0.016 g, 0.2 mmol), 4-bpfp (0.032 g, 0.1 mmol), H_2O (12 mL) and NaOH (0.014 g, 0.35 mmol) was stirred for 30 min in air and then transferred and sealed in a 25 mL Teflon reactor, which was heated at 120 °C for 4 d, leading to the formation of blue block-shaped crystals. These were washed with water and dried in air. Yield: ∼ 25 % (based on Cu). – Anal. for $C_{13}H_{16}CuN_2O_6$: calcd. C 43.36, H 4.45, N 7.78; found C 43.44, H 4.37, N 7.71 %. – IR (KBr, cm^{-1}): ν = 3564 m, 3503 m, 3075 w, 2986 w, 2931 m, 2863 m, 2373 w, 1625 s, 1550 m, 1503 w, 1421 s, 1354 m, 1313 s, 1279 s, 1251 s, 1210 w, 1156 m, 1054 m, 1003 s, 966 w, 905w , 878 m, 843 s, 788 m, 761 m, 734 m, 707 m, 680 w, 646 s, 571 m, 517 s.

X-Ray crystallographic study

Crystallographic data for complexes **1** and **2** were collected on a Bruker APEX area-detector diffractometer with

Table 1. Crystal data and and numbers pertinent to data collection and structure refinement for complexes **1** and **2**.

Empirical formula	$C_{30}H_{26}Cu_2N_6O_{12}$	$C_{13}H_{16}CuN_2O_6$
Formula wt.	789.67	359.82
Crystal size, mm^3	0.16 × 0.15 × 0.12	0.19 × 0.15 × 0.14
Crystal system	triclinic	monoclinic
Space group	$P\bar{1}$	$P2_1/c$
T, K	293(2)	293(2)
a, Å	7.235(5)	13.5920(15)
b, Å	10.494(5)	13.1870(15)
c, Å	11.006(5)	8.585(1)
α, deg	65.531(5)	90
β, deg	79.141(5)	107.940(1)
γ, deg	74.811(5)	90
V, $Å^3$	731.0(7)	1463.9(3)
Z	1	4
$D_{calcd.}$, g cm^{-3}	1.79	1.63
μ(MoK_α), mm^{-1}	1.5	1.5
F(000), e	402	740
hkl range	−2 → 9, −13 → 11, ±14	−16 → 15, −15 → 10, ±10
θ_{max}, deg	27.70	24.99
Refl. measd / unique / R_{int}	12322 / 3445 / 0.0204	7180 / 2576 / 0.0276
R_1 / wR_2 (all data)	0.0331 / 0.1273	0.0469 / 0.1097
GOF	1.098	1.090
$\Delta\rho_{max/min}$, e $Å^{-3}$	0.65 / −0.65	1.17 / −0.51

Table 2. Selected bond lengths (Å) and angles (deg) for complexes **1** and **2**[a].

1			
Cu(1)–O(2)	2.0324(18)	Cu(1)–O(1W)	2.224(2)
Cu(1)–N(1)	1.9773(19)	Cu(1)–O(5)	2.0392(18)
Cu(1)–N(2)	1.9071(19)		
N(2)–Cu(1)–N(1)	167.95(8)	N(1)–Cu(1)–O(1W)	92.38(8)
N(2)–Cu(1)–O(2)	80.30(8)	O(2)–Cu(1)–O(1W)	94.45(7)
N(1)–Cu(1)–O(2)	100.70(7)	O(5)–Cu(1)–O(1W)	98.87(8)
N(2)–Cu(1)–O(5)	80.08(8)	O(2)–Cu(1)–O(5)	157.83(7)
N(1)–Cu(1)–O(5)	96.38(8)	N(2)–Cu(1)–O(1W)	99.53(9)
2			
Cu(1)–O(3)#1	1.961(2)	Cu(1)–O(2)#3	1.980(2)
Cu(1)–O(4)#2	1.971(2)	Cu(1)–N(1)	2.163(3)
Cu(1)–O(1)	1.976(2)	N(1)–Cu(1)–Cu(1)#3	175.04(8)
O(3)#1–Cu(1)–O(4)#2	168.14(10)	O(3)#1–Cu(1)–O(1)	88.49(11)
O(4)#2–Cu(1)–O(1)	91.16(11)	O(3)#1–Cu(1)–O(2)#3	90.43(10)
O(4)#2–Cu(1)–O(2)#3	87.52(11)	O(1)–Cu(1)–O(2)#3	168.30(10)
O(3)#1–Cu(1)–N(1)	94.30(10)	O(1)–Cu(1)–N(1)	95.02(10)
O(4)#2–Cu(1)–N(1)	97.54(10)	O(2)#3–Cu(1)–N(1)	96.69(10)
O(3)#1–Cu(1)–Cu(1)#3	81.45(7)	O(4)#2–Cu(1)–Cu(1)#3	86.75(7)
O(1)–Cu(1)–Cu(1)#3	82.36(7)	O(2)#3–Cu(1)–Cu(1)#3	85.96(7)

[a] Symmetry codes for **2**: #1 x, $-y+1/2$, $z-1/2$; #2 $-x+1$, $y-1/2$, $-z+5/2$; #3 $-x+1$, $-y$, $-z+2$.

Table 3. Hydrogen bonding parameters (Å, deg) for complex **1**[a].

D–H···A	D–H	H···A	D···A	D–H···A
O(1W)–H(1WA)···O(1)#2	0.85(4)	2.18(4)	2.808(3)	131(3)
O(1W)–H(1B)···O(4)#3	0.85(4)	1.98(3)	2.716(3)	145(4)
C(14)–H(14A)···O(3)#4	0.93(3)	2.48(3)	3.211(4)	136(4)

[a] Symmetry codes: #2 $-x$, $-y$, $1-z$; #3 $-x$, $-y$, $-z$; #4 $1+x$, $-1+y$, $1+z$.

MoK_α radiation ($\lambda = 0.71069$ Å) in ω scan mode. The structures were solved by Direct Methods using the SHELXS program of the SHELXTL package and refined by full-matrix least-squares methods with SHELXL [35–37]. All non-hydrogen atoms were refined anisotropically. The hydrogen atoms of the ligands were generated geometrically and refined isotropically with fixed displacement parameters. For **2**, the hydrogen atoms of the water molecules could not be located. A summary of crystal data and structure refinements for the two complexes are provided in Table 1. Selected bond lengths and angles are listed in Table 2. The related hydrogen bonding geometries of **1** are given in Table 3.

CCDC 884245 (**1**) and 884246 (**2**) contain the supplementary crystallographic data for the paper. These data can be obtained free of charge from The Cambridge Crystallographic Data Centre *via* www.ccdc.cam.ac.uk/data_request/cif.

Acknowledgement

The supports by the National Natural Science Foundation of China (no. 20871022 and 21171025), New Century Excellent Talents in University (NCET-09-0853), the Natural Science Foundation of Liaoning Province (no. 201102003), and the Program of Innovative Research Team in University of Liaoning Province (LT2012020) are gratefully acknowledged.

[1] J. Tao, J. X. Shi, M. L. Tong, X. X. Zhang, X. M. Chen, *Inorg. Chem.* **2001**, *40*, 6328–6330.
[2] C. Qin, X. L. Wang, Y. G. Li, E. B. Wang, Z. M. Su, L. Xu, R. Clerac, *Dalton Trans.* **2005**, 2609–2614.
[3] J. Zhang, Y. B. Chen, S. M. Chen, Z. J. Li, J. K. Cheng and Y. G. Yao, *Inorg. Chem.* **2006**, *45*, 3161–3163.
[4] L. Xu, G. C. Guo, B. Liu, M. S. Wang, J. S. Huang, *Inorg. Chem. Commun.* **2004**, *7*, 1145–1149.
[5] N. N. Adarsh, D. K. Kumar, P. Dastidar, *Cryst. Growth Des.* **2009**, *9*, 2979–2983.
[6] J. Yang, J. F. Ma, Y. Y. Liu, J. C. Ma, S. R. Batten, *Inorg. Chem.* **2007**, *46*, 6542–6555.
[7] L. S .Wang, L. Zhu, P. C. Yin, Y. G. Wei, *Inorg. Chem.* **2009**, *48*, 9222–9235.
[8] X. L. Wang, Y. F. Bi, G. C. Liu, H. Y. Lin, T. L. Hu, X. H. Bu, *CrystEngComm* **2008**, *10*, 349–356.

[9] M. Eddaoudi, J. Kim, J. B. Wachter, H. K. Chae, M. O'Keeffe, O. M. Yaghi, *J. Am. Chem. Soc.* **2001**, *123*, 4368 – 4369.
[10] X. G. Wang, J. Li, B. Ding, E. C. Yang, X. J. Zhao, *J. Mol. Struct.* **2008**, *876*, 268 – 277.
[11] D. S. Deng, P. Liu, W. J. Fu, L. Li, F. X. Yang, B. M. Ji, *Inorg. Chim. Acta* **2010**, *363*, 891 – 899.
[12] K. L. Hou, F. Y. Bai, Y. H. Xing, J. L. Wang, Z. Shi, *Inorg. Chim. Acta* **2011**, *365*, 269 – 276.
[13] L. Gou, Z. X. Han, H. M. Hu, Q. R. Wu, X. L. Yang, Z. H. Yang, B. C. Wang, F. Wang, M. L. Yang, G. L. Xue, *Inorg. Chim. Acta* **2010**, *363*, 2590 – 2599.
[14] T. Duangthongyou, C. Phakawatchai, S. Siripaisarnpipat, *J. Mol. Struct.* **2011**, *987*, 101 – 105.
[15] M. R. Montney, R. M. Supkowski, R. J. Staples, R. L. LaDuca, *J. Solid State Chem.* **2009**, *182*, 8 – 17.
[16] L. S. Long, Y. R. Wu, R. B. Huang, L. S. Zheng, *Inorg. Chem.* **2004**, *43*, 3798 – 3800.
[17] B. Chen, C. Liang, J. Yang, D. S. Contreras, Y. L. Clancy, E. B. Lobkovsky, O. M. Yaghi, S. Dai, *Angew. Chem. Int. Ed.* **2006**, *45*, 1390 – 1393.
[18] T. Duangthongyou, S. Jirakulpattana, C. Phakawatchai, M. Kurmoo, S. Siripaisarnpipat, *Polyhedron* **2010**, *29*, 1156 – 1162.
[19] X. L. Wang, J. Li, H. Y. Lin, H. L. Hu, B. K. Chen, B. Mu, *Solid State Sci.* **2009**, *11*, 2118 – 2124.
[20] X. L. Wang, H. Y. Lin, B. Mu, A. X. Tian, G. C. Liu, *Dalton Trans.* **2010**, *39*, 6187 – 6189.
[21] X. L. Wang, B. Mu, H. Y. Lin, G. C. Liu, *J. Organomet. Chem.* **2011**, *696*, 2313 – 2321.
[22] H. Y. Lin, B. Mu, X. L. Wang, A. X. Tian, *J. Organomet. Chem.* **2012**, *702*, 36 – 44.
[23] X. L. Wang, B. Mu, H. Y. Lin, G. C. Liu, A. X. Tian, S. Yang, *CrystEngComm* **2012**, *14*, 1001 – 1009.
[24] X. L. Wang, B. Mu, H. Y. Lin, G. C. Liu, A. X. Tian, J. Li, Z. H. Kang, *Transition Met. Chem.* **2010**, *35*, 967 – 971.
[25] X. L. Wang, H. Y. Lin, B. Mu, A. X. Tian, G. C. Liu, N. H. Hu, *CrystEngComm* **2011**, *13*, 1990 – 1999.
[26] J. S. Lucas, A. L. Pochodylo, R. L. LaDuca, *CrystEngComm* **2010**, *12*, 3310 – 3317.
[27] C. Y. Wang, Z. M. Wilseck, R. M. Supkowski, R. L. LaDuca, *CrystEngComm* **2011**, *13*, 1391 – 1399.
[28] Z. M. Wilseck, C. M. Gandolfo, R. L. LaDuca, *Inorg. Chim. Acta* **2010**, *363*, 3865 – 3873.
[29] A. Banisafar, R. L. LaDuca, *Inorg. Chim. Acta* **2011**, *373*, 295 – 300.
[30] Z. M. Wilseck, R. L. LaDuca, *Inorg. Chem.Commun.* **2011**, *14*, 706 – 710.
[31] C. M. Gandolfo, R. L. LaDuca, *Cryst. Growth Des.* **2011**, *11*, 1328 – 1337.
[32] X. L. Wang, H. Y. Zhao, H. Y. Lin, G. C. Liu, J. N. Fang, B. K. Chen, *Electroanalysis* **2008**, *20*, 1055 – 1060.
[33] R. Meng, S. G. Weber, *J. Electroanal. Chem.* **2007**, *600*, 325 – 334.
[34] H. W. Hou, Y. L. Song, H. Xu, Y. L. Wei, Y. T. Fan, Y. Zhu, L. K. Li, C. X. Du, *Macromolecules* **2003**, *36*, 999 – 1003.
[35] G. M. Sheldrick, SHELXS/L-97, Programs for Crystal Structure Determination, University of Göttingen, Göttingen (Germany) **1997**.
[36] G. M. Sheldrick, *Acta Crystallogr.* **1990**, *A46*, 467 – 473.
[37] G. M. Sheldrick, *Acta Crystallogr.* **2008**, *A64*, 112 – 122.